ARTIFICIAL NEURAL NETWORK ASSISTED MULTI-OBJECTIVE OPTIMIZATION OF A METHANE-FED DIR-SOFC SYSTEM WITH WASTE HEAT RECOVERY

by

Unsal AYBEK[a*], Lutfu NAMLI[b], Mustafa OZBEY[b], and Bekir DOGAN[a]

[a] Tokat Vocational School, Tokat Gaziosmanpasa University, Tokat, Turkey
[b] Faculty of Engineering, Ondokuz Mayis University, Samsun, Turkey

Original scientific paper
https://doi.org/10.2298/TSCI2304413A

The main purpose of this study is to enhance the performance of solid oxide fuel cell systems. For this purpose, a mathematical model of a direct internal reforming (DIR) methane-fed solid oxide fuel cell system with waste heat recovery was designed in the engineering equation solver program. We optimised the performance of the solid oxide fuel cell using a genetic algorithm and TOPSIS technique considering exergy, power, and environmental analyzes. An ANN working with the Levenberg-Marquardt training function was designed in the MATLAB program to create the decision matrix to which the TOPSIS method will be applied. According to the power optimization, 786 kW net power was obtained from the system. In exergetic optimization, the exergy efficiency was found to be 57.6%. In environmental optimization, the environmental impact was determined as 330.6 kgCO_2/MWh. According to the multi-objective optimization results, the exergy efficiency, the net power of the solid oxide fuel cell system, and the environmental impact were 504.1 kW, 40.08%, and 475.4 kgCO_2/MWh.

Key words: *ANN, clean energy, Levenberg-Marquardt, multi-objective optimization, solid oxide fuel cell*

Introduction

Fuel cells are a chemical fuel device capable of converting the chemical energy directly into electrical energy using an electrochemical reaction, a highly efficient and environmentally friendly energy source since no combustion is required. The FC are also seen as promising future clean energy technologies due to the natural advantages of electrochemical conversion compared to thermal combustion systems [1, 2]. Solid oxide fuel cells (SOFC) have desirable energy conversion efficiency and expanded fuel flexibility with little environmental impact (EMI) [3]. A single-cell component of the SOFC consists of a homogenous layer made of electrode materials and electrolytes, and the electrolyte layer is sandwiched between the anode and the cathode [4]. The anode material, the cathode material, and the solid electrolyte are generally made of zirconia and nickel, strontium-doped lanthanum manganite ($La_{0.84}Sr_{0.16}$), and yttrium-stabilised zirconia, respectively [5, 6]. The SOFC operating principle is based on semi-electro reactions at the electrodes.

* Corresponding author, e-mail: unsal.aybek@gop.edu.tr

Optimization of SOFC is a critical approach that can decline costs and develop efficiency [7]. For several years, many papers have been carried out to improve the performance, efficiency, and reliability of SOFC. The Red Fox optimization (IRFO) algorithm, which was developed to determine the most suitable model for a SOFC system, was used by Zhang *et al*. [8]. In this article study, it was reported that the ELM-IRFO method had a minimum value of MSE when compared with the Grey Wolf Optimization-Rotor Hopfield Neural Network (GWO-RHNN) method in [8]. Chen *et al.* [7] designed an ANN to optimise the SOFC parameters, which contain anode layer porosity, cathode layer thickness, and electrolyte layer thickness, using the GWO. Subotić *et al.* [9] designed ANN to predict the SOFC performance and validated the performance of the SOFC by combining experimental data and two physical models. A combination of SOFC-Rankine cycle-Kalina cycle (SOFC-RC-KC) energy systems to recover waste heat was proposed by Song *et al*. [10]. They created a Duran-Grassmann optimization model and optimised the operating parameters using a GA to enhance the power generation of this system. Bai and Li [11] have evaluated the SOFC model parameter using a hybrid algorithm, which is acquired from the integration of GWO and cuckoo search algorithms. Yousri *et al*. [12] analyzed the parameters of the SOFC using the marine predator algorithm. The results showed that this algorithm provided highly accurate identified parameters.

In this study, we aimed to improve the system performance of the SOFC system. To improve methane-fed SOFC system with waste heat recovery performance thermodynamically, voltage, power, exergy, and emission analyzes were performed by changing the key parameters. Also, multi-objective optimization was used to achieve the optimum performance of the designed system concerning three objectives: high net power, low emission rate, and high exergy efficiency.

System description

The air and fuel are separately compressed and preheated in the respective preheaters with the aid of the exhaust gases. Similarly, after the water pump pressurises the water, it is preheated to produce superheated steam in the heat exchanger using the heat from the exhaust gases from the afterburner, and then the superheated steam is mixed with the compressed fuel to perform the internal reforming reaction. While the preheated air is delivered to the cathode, the fuel and steam mixture is sent to the anode side of this system, where an electrochemical reaction takes place between the mixture and the air. The electrochemical reaction is converted by an inverter to alternating current with the module of direct current electricity to store. Excess air departs the cathode out the stack exit, while unreacted fuel exits by the anode. These two outlet streams are mixed and fully combusted in the afterburner, where the exhaust gas is used to preheat the fuel, water, and air. The schematic diagram of a DIR-SOFC system where exhaust gases are evaluated in the afterburner is shown in fig. 1. The material and structure of SOFC are decisive factors in its maximum temperature gradient. In the literature, the safe temperature gradient for the SOFC is 10 K/cm [13]. In 0.1 m × 0.1 m active surface area, the maximum temperature difference between the fuel cell inlet and outlet can be accepted as 100 °C [14]. Nickel (Ni) and Y_2O_3-stabilized zirconia catalyse steam methane reforming at high temperatures, usually 700 °C to 900 °C [15].

This study performed analyzes under steady-state conditions and in thermodynamic equilibrium. Potential and kinetic energy changes were ignored. The SOFC system is modelled according to the assumptions stated in [14, 16].

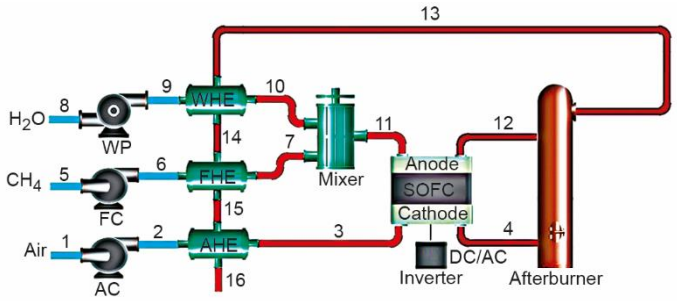

Figure 1. Schematic of a methane-fed DIR-SOFC system with waste heat recovery

Modelling of reformer and thermodynamic evaluation

The SOFC model to simultaneously utilise H_2 and CO, thus contributing to energy generation. Through DIR inside the fuel cell, methane, and CO result as a fuel mixture. For the reforming, shifting, and electrochemical processes, the molar conversion rates are x_r, y_r, and z_r, respectively. These chemical reactions take place in the anode and cathode electrodes of the fuel cell as shown in eqs. (1)-(3) [16-19]:

$$x_r \rightarrow [CH_4 + H_2O \rightarrow CO + 3H_2] \text{ (Reforming)} \tag{1}$$

$$y_r \rightarrow [CO + H_2O \rightarrow CO_2 + H_2] \text{ (Shifting)} \tag{2}$$

$$z_r \rightarrow [H_2 + \frac{1}{2}O_2 \rightarrow H_2O] \text{ (Overall electrochemical reaction)} \tag{3}$$

The air utilisation factor and the fuel utilisation factor, respectively, are defined in:

$$U_a = \frac{(\text{Air})_{\text{consumed}}}{(\text{Air})_{\text{supplied}}} = \frac{(O_2)_{\text{consumed}}}{(O_2)_{\text{supplied}}} = \frac{\frac{z_r}{2}}{\dot{n}_{O_{2,3}}} \tag{4}$$

$$U_f = \frac{(\text{Fuel})_{\text{consumed}}}{(\text{Fuel})_{\text{supplied}}} = \frac{(H_2)_{\text{consumed}}}{(H_2)_{\text{supplied}}} = \frac{z_r}{3x_r + y_r} \tag{5}$$

The constants of x_r and y_r are obtained by the equilibrium constant and current relations. The K_S shift is the equilibrium constant for shift reaction, which is expressed as:

$$lnK_S = -\frac{\Delta\bar{g}_s^o}{\bar{R}T_{FC,e}} = \ln\left[\frac{y_r(3x_r + y_r - z_r)}{(x_r - y_r)(1.5x_r - y_r + z_r)}\right] \tag{6}$$

The latter quantity is defined:

$$\Delta\bar{g}_s^o = \bar{g}_{s,CO_2}^o + \bar{g}_{s,H_2}^o - \bar{g}_{s,H_2O}^o - \bar{g}_{s,CO}^o, \quad \bar{g}_s^o = \bar{h} - T_{FC,e}\bar{s}^o \tag{7}$$

The resulting current I and current density j are defined:

$$I = jA_a, \quad j = \frac{2Fz_r}{N_{FC}A_a} \tag{8}$$

where N_{FC}, F, and A_a, are the cell number, Faraday constant, and the effective surface area, respectively, $\dot{W}_{\text{SOFC, stack}}$ – the work rate produced by the SOFC stack, V_{Cell} – the cell voltage, V_{N} – the Nernst voltage, and V_{Loss} – the sum of the different voltage losses (ohm – ohmic, act – activation, and conc – concentration). These can be written in eq. (9), respectively:

$$\dot{W}_{\text{SOFC,stack}} = N_{FC} I V_{\text{Cell}}, \quad V_{\text{Cell}} = V_{\text{N}} - V_{\text{Loss}}, \quad V_{\text{Loss}} = V_{\text{ohm}} + V_{\text{act}} + V_{\text{conc}} \tag{9}$$

At a steady-state, an energy rate balance for a system component (ignore any changes in potential and kinetic energy) can be written:

$$\dot{Q} - \dot{W} = \sum_i \dot{n}_i \bar{h}_i - \sum_e \dot{n}_e \bar{h}_e \tag{10}$$

where $\dot{Q}$ denotes the heat transfer rate, $\dot{W}$ denotes work transfer rate, and $\bar{h}$ denotes molar enthalpy [14, 16, 18].

The exergy of a system is the sum of its physical, potential, kinetic and chemical exergies. A reduction in total exergy destruction, which promotes process efficiency, increases the system energy:

$$\dot{E}x = \dot{E}x^{ph} + \dot{E}x^{ch} \tag{11}$$

$$\dot{E}x^{ph} = \sum_i \dot{n}_i (\bar{h}_i - \bar{h}_0) - T_0 (\bar{s}_i - \bar{s}_0), \quad \dot{E}x^{ch} = \dot{n} \left(\sum_i y_i \overline{ex}_i^{ch,0} - \bar{R} T_0 \sum_i y_i \ln y_i \right) \tag{12}$$

where $\bar{s}$ is the molar entropy and $\overline{ex}_i^{ch,0}$ is the standard chemical exergy of a species. Exergy efficiency definitions and equations for the SOFC system [16, 18, 20]. The exergy efficiency calculations for the SOFC system can be written:

$$\dot{E}x_{\text{in}} = \dot{n}_{\text{CH}_{4,11}} \overline{ex}_{\text{CH}_4}^{ch,0}, \quad \eta_{II} = [\dot{W}_{SOFC;ac} - (\dot{W}_{ac} + \dot{W}_{fc} + \dot{W}_{wp})] \frac{100}{\dot{E}x_{\text{in}}} \tag{13}$$

Due to the prevailing flow rate of the CO_2 in the exhaust gases compared with other harmful gases, the EMI of the suggested system was determined by the EMI factor [21, 22]. This factor is expressed:

$$EMI = \frac{\dot{m}_{\text{co}_2}}{\dot{W}_{\text{net}}} 3.6 \cdot 10^6 \tag{14}$$

Multi-criteria decision-making of TOPSIS method

The TOPSIS method determines the best solution by calculating the relative closeness coefficient for all alternatives. The normalized decision matrix, the weighted normalized matrix are expressed by eq. (15) respectively:

$$D = \begin{bmatrix} x_{11} & \cdots & x_{1n} \\ \vdots & \ddots & \vdots \\ x_{m1} & \cdots & x_{mn} \end{bmatrix}, \quad y_{ij} = \frac{x_{ij}}{\sqrt{\sum_{k=1}^{m} x_{kj}^2}}, \quad v_{ij} = y_{ij} w_{ij} \tag{15}$$

The ideal, P^+, and negative-ideal, P^-, solutions are obtained using eqs. (16) and (17), respectively:

$$P^+ = \{v_1^+, \ldots, v_n^+\} = \{(\max_j v_{ij} \,|\, i \in R'\}, \{(\max_j v_{ij} \,|\, i \in R''\}, \{(\min_j v_{ij} \,|\, i \in R'''\} \tag{16}$$

$$P^- = \{v_1^-, \ldots, v_n^-\} = \{(\min_j v_{ij} \,|\, i \in R'\}, \{(\min_j v_{ij} \,|\, i \in R''\}, \{(\max_j v_{ij} \,|\, i \in R'''\} \tag{17}$$

where R' is the system's net power, R'' – the exergy efficiency, and R''' – the EMI factor.

Each alternative gap from the positive, D_j^+, and negative, D_j^-, ideal solutions is determined. The proximity coefficient for each choice is determined in the last stage. The higher values of C were used to determine the order of the options [19, 23]:

$$D_j^+ = \sqrt{\sum_{i=1}^{n}(v_{ij} - v_i^+)^2}, \quad D_j^- = \sqrt{\sum_{i=1}^{n}(v_{ij} - v_i^-)^2}, \quad C = \frac{D_j^-}{D_j^+ + D_j^-} \tag{18}$$

Validation of the SOFC model

Tao *et al.* [24] provided experimental findings using methane as fuel and theoretical data presented by Colpan *et al.* [14] and Chitsaz *et al.* [18] were used to verify the results of the model used in this study, tab. 1. The experimental results showed a maximum difference of ±4.41% in cell voltage and ±4.89% in power density. It is considered that this difference is mainly due to the assumptions taken into account in the current model. In addition, it was seen that the present study was compatible with other theoretical studies in the mentioned literature.

Table 1. Comparison of the present model with experimental and theoretical data in the literature

Current density [Acm^{-2}]	Cell voltage [V]/Power density [Wm^{-2}]							
	Present model		Experimental model [24]		Theoretical model [14]		Theoretical model [18]	
0.1	0.855	0.086	0.86	0.082	0.83	0.083	–	–
0.2	0.782	0.156	0.76	0.15	0.794	0.159	0.79	0.158
0.3	0.71	0.213	0.68	0.21	0.753	0.226	0.711	0.216
0.4	0.64	0.256	0.62	0.26	0.705	0.282	0.644	0.253
0.5	0.572	0.286	0.57	0.295	0.639	0.319	0.56	0.288
0.6	0.505	0.303	0.52	0.315	0.57	0.342	0.51	0.3

Results and discussion

Effects of design parameters on system performance

System performances were investigated in the operating ranges of selected desing parameters (current density 2500-20000 A/m^2, operating temperature 750-1000 °C and fuel utilisation factor 0.6-0.9). When the effect of the relevant design parameters was not examined, the current density was fixed at 8000 A/m^2, the operating temperature was 750 °C and the fuel utilisation factor was 0.7. Literature was taken as a basis for other cell characteristics [14, 16]. Figure 2 shows the effect of design parameters on performance parameters.

The increase in current density caused an increase in voltage losses and a corresponding decrease in cell voltage. Therefore, it is expected that the electrical power obtained from the SOFC will increase up to a certain current density and then decrease. The increase in net power up to the optimum current point remained below the increase in exergy destruction with the increasing current density. Thus, as the current density increased, the exergy efficiency of the system decreased, and this decrease accelerated when the optimum current density was exceeded. The fact that the rate of increase in CO_2 emissions up to the optimum current density was higher than the rate of increase in the net power of the system caused the EMI to increase, and the acceleration in this direction increased after the optimum current density.

When the operating temperature was increased, activation and concentration voltage losses increased. But, ohmic losses and Nernts voltage decreased. With the decrease of the cell voltage, there is a decrease in the electrical power and net power obtained from the SOFC. In addition, there are an increase in the exergy destruction and a decrease in the exergy efficiency of the system. Depending on this increase in the operating temperature, the CO_2 emissions along with the CH_4 mass-flow rate increased, and as a result, the EMI increased.

The increase in the fuel utilisation factor decreased the Nernts voltage, increased the concentration losses in the anode region and thus decreased the cell voltage and also reduction in fuel and water vapour demand decreased the power drawn by the fuel compressor and water pump. However the system net power decreased as the rate of decrease of the electrical power obtained from the SOFC was higher. With the decrease in net power, the decrease in fuel input increased the exergy efficiency up to about 0.85 U_f and then decreased it. The opposite situation was observed in EMI.

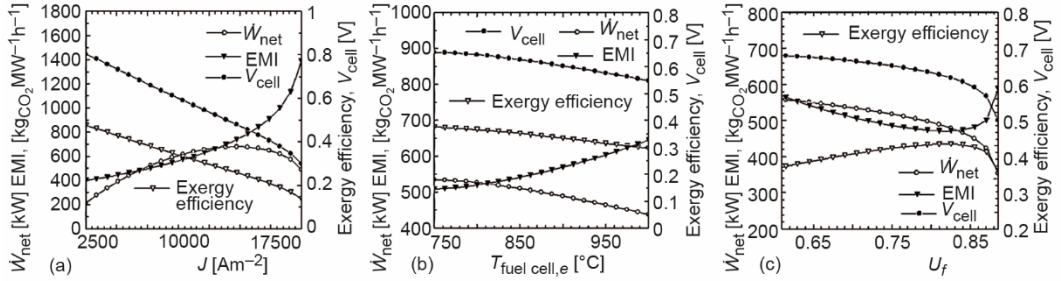

Figure 2. Effect of (a) current density, (b) operating temperature, and (c) fuel utilisation factor on system performance

Optimizations of the system

The most crucial aim of the study was to obtain maximum power and efficiency from the system and to realize minimum emissions. For this purpose, the system net power, exergy efficiency and EMI factor were considered objective functions. In this study, single objective optimizations for each purpose were carried out with the GA method in the engineering equation solver (EES) program, in which the mathematical model was created. Optimization results in the intervals determined for the design parameters are given in tab. 2.

A wide-range matrix was created between the design parameters boundaries to approach the optimum solution point and multi-objective optimization was performed on this matrix. This matrix was solved in the EES program, the solution table was transferred to the

MATLAB program, and the TOPSIS decision-making method was applied to the results. While using the TOPSIS method, equal weights of 1/3 were given to each objective function. The best optimum solution point of the wide-range matrix is shown in tab. 3. The design parameters lower limit and the upper limit at the best solution point calculated in tab. 3. were determined as the optimum solution region. As shown in tab. 4. a training matrix and a simulation matrix were created by narrowing the matrix intervals. The training matrix was solved in the EES program, and the solution table was transferred to the MATLAB program and used in the training of ANN.

Table 2. Optimal values of design and performance parameters according to single objective optimization results

Design parameter	Power optimization	Exergetic optimization	Environmental optimization
J [Am^{-2}]	17611	2502	2502
$T_{\text{fuel cell},e}$ [°C]	787.7	751.6	750.6
U_f	0.6001	0.90	0.8997
Performance parameter			
$\dot{W}_{\text{net}}$ [kW]	786	193.1	193.3
η_{II}	0.2089	0.576	0.576
EMI [kgCO_2 per MWh]	911.9	330.8	330.6

Table 3. Multi-objective optimization on wide-range matrix

Design parameter	Lower limit	Upper limit	Matrix range	The best solution in the matrix range
J [Am^{-2}]	2500	20000	500	8000
$T_{\text{fuel cell},e}$ [°C]	750	1000	50	750
U_f	0.6	0.90	0.05	0.75
Performance parameter				
$\dot{W}_{\text{net}}$ [kW]				517.8
η_{II}				0.392
EMI [kgCO_2 per MWh]				486

Table 4. The training and simulation matrix for ANN

Design parameter	Lower limit	Upper limit	Training matrix range	Simulation matrix range
J [Am^{-2}]	7500	8500	100	1
$T_{\text{fuel cell},e}$ [°C]	750	800	10	1
U_f	0.7	0.8	0.0125	0.005

In ANN training, a feed-forward backdrop was preferred as the neural network type. As training, adaption learning, performance, and transfer functions, TRAINLM, LEARNGDM, MSE, and TANSIG were employed. The designed ANN model is shown in fig. 3.

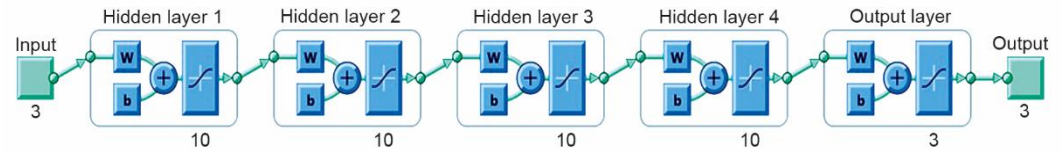

Figure 3. The ANN model designed for the DIR-SOFC training

The designed neural network is given a dataset of 594 rows, and the performance curves are shown in fig. 4(a). According to the MSE method, the best validation performance was 0.00097235 at epoch 707. As shown in fig. 4(b), the *R* value was found to be 1 in all network procedures. The analysis showed that the model training, testing and validation network procedures were significantly valid.

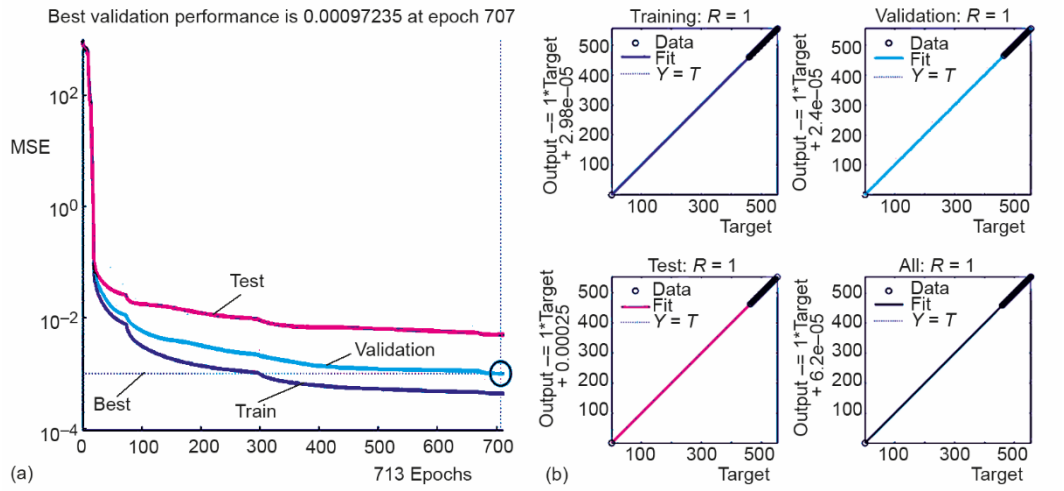

Figure 4. (a) The best validation performance and (b) the regression analysis of the ANN model

The error percent between the target outputs obtained from the ANN model and the actual target outputs in the training dataset is shown in fig. 5. It was observed that there was a maximum error of 0.0018% in system net power, 0.0066% in exergy efficiency, and 0.0009% in EMI. These errors were found to be negligible for all targets. The simulation matrix created in tab. 4 was simulated in the ANN model, and the TOPSIS decision-making method was applied to the target outputs. A common optimum solution point was determined for all target outputs. The findings obtained from the ANN model at the optimum point were checked in the EES program, and a minimum 99.6% similarity was found between the target outputs. The results are presented in tab. 5.

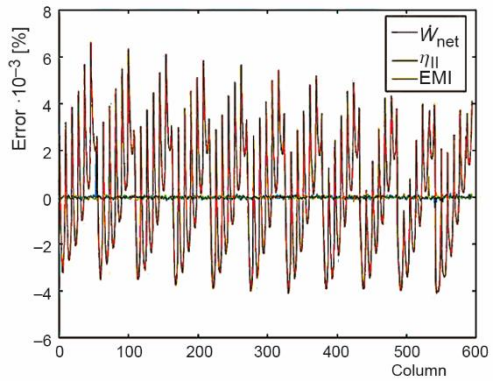

Figure 5. Errors between the ANN outputs and actual outputs

Table 5. Multi-objective optimization results using the Topsis method

Design parameter	Multi-objective optimization		
J [Am^{-2}]	7850		
$T_{\text{fuel cell},e}$ [°C]	750		
U_f	0.77		
Performance parameter	ANN	EES	Error [%]
$\dot{W}_{\text{net}}$ [kW]	504.1094	504.1	0.0018
η_{II}	0.3992	0.4008	–0.399
EMI [kgCO_2 per MWh]	475.3548	475.4	–0.00951

Conclusions

The essential objective of this work was to improve the performance of the SOFC. In this study, a mathematical model of a DIR methane-fed SOFC system was designed in the EES version 9.457-3D software. The performance of SOFC was optimised using a GA and TOPSIS technique considering exergy, power and environmental analyzes. According to the power optimization, 786 kW net power was obtained from the system. In exergetic optimization, the exergy efficiency was found to be 57.6%. In environmental optimization, the EMI was determined as 330.6 kgCO_2/MWh. According to the multi-objective optimization results, the system's net power, the exergy efficiency, and the EMI were 504.1 kW, 40.08%, and 475.4 kgCO_2/MWh. The findings obtained from the ANN model at the optimum point were checked in the EES program, and a minimum 99.6% similarity was found between the target outputs. It has been seen that the target outputs of the selected ANN model are compatible with the actual outputs, and it is a good choice for creating a decision matrix. In addition to choosing the ANN model, obtaining an approximate solution region before the model is created allows for reaching the optimum point with few errors.

References

[1] Stambouli, A. B., Fuel cells: The Expectations for an Environmental-Friendly and Sustainable Source of Energy, *Renewable and Sustainable Energy Reviews, 15* (2011), 9, pp. 4507-4520
[2] Singh, M., *et al*., Solid Oxide Fuel Cell: Decade of Progress, Future Perspectives and Challenges, *International Journal of Hydrogen Energy*, *46* (2021), 54, pp. 27643-27674
[3] Hussain, S., Yangping, L., Review of Solid Oxide Fuel Cell Materials: Cathode, Anode, and Electrolyte, *Energy Transit, 4* (2020), Oct., pp. 113-126

[4] Raza, T., *et al*., Recent Advance in Physical Description and Material Development for Single Component SOFC: A mini-review, *Chemical Engineering Journal*, *444* (2022), Sept., 136533
[5] Song, S., *et al*., Modeling the SOFC by BP Neural Network Algorithm, *International Journal of Hydrogen Energy*, *46* (2021), 38, pp. 20065-20077
[6] Diaz-Aburto, I., *et al*., Mo, Cu-doped CeO_2 as Anode Material of Solid Oxide Fuel Cells (SOFC) using Syngas as Fuel, *J. Electrochem. Sci. Technol*, *12* (2023), 2, pp. 246-256
[7] Chen, X., *et al*., Artificial Neural Network Modeling and Optimization of the Solid Oxide Fuel Cell Parameters using Grey Wolf Optimiser, *Energy Reports*, *7* (2021), Nov., pp. 3449-3459
[8] Zhang, M., *et al*., An Optimal Model Identification for Solid Oxide Fuel Cell Based on Extreme Learning Machines Optimised by improved Red Fox Optimization Algorithm, *International Journal of Hydrogen Energy*, *46* (2021), 55, pp. 28270-28281
[9] Subotić, V., *et al*., Artificial Intelligence for Time-Efficient Prediction and Optimization of Solid Oxide Fuel Cell Performances, *Energy Conversion and Management*, *230* (2021), Feb., 113764
[10] Song, M., *et al*., Thermodynamic Performance Assessment of SOFC-RC-KC System for Multiple Waste Heat Recovery, *Energy Conversion and Management*, *245* (2021), Oct., 114579
[11] Bai, Q., Li, H., The Application of Hybrid Cuckoo Search-Grey Wolf Optimization Algorithm in Optimal Parameters Identification of Solid Oxide Fuel Cell, *International Journal of Hydrogen Energy*, *47* (2022), 9, pp. 6200-6216
[12] Yousri, D., *et al*., Parameters Identification of Solid Oxide Fuel Cell for Static and Dynamic Simulation using Comprehensive Learning Dynamic Multi-Swarm Marine Predators Algorithm, *Energy Conversion and Management*, *228* (2021), Jan., 113692
[13] Wu, X., *et al*., Temperature Gradient Control of a Solid Oxide Fuel Cell Stack, *Journal of Power Sources*, *414* (2019), Feb., pp. 345-353
[14] Colpan, C. O., *et al*., Thermodynamic Modeling of Direct Internal Reforming Solid Oxide Fuel Cells Operating with Syngas, *International Journal of Hydrogen Energy*, *32* (2007), 7, pp. 787-795
[15] Li, H., Carbon Deposition on Ni/YSZ anode SOFC for Direct Methane Steam Reforming, Graduate Theses, Dissertations, and Problem Reports, 4070, West Virginia University, Morgantown, West Virginia, 2019
[16] Ranjbar, F., *et al*., Energy and Exergy Assessments af a Novel Trigeneration System Based on a Solid Oxide Fuel Cell, *Energy Conversion and Management*, *87* (2014), Nov., pp. 318-327
[17] Chan, S. H., *et al*., Modelling of Simple Hybrid Solid Oxide Fuel Cell and Gas Turbine Power Plant, *Journal of Power Sources*, *109* (2002), 1, pp. 111-120
[18] Chitsaz, A., *et al*., Effect of Recycling on The Thermodynamic and Thermoeconomic Performances of SOFC Based on Trigeneration Systems; A comparative study, *Energy*, *124* (2017), Apr., pp. 613-624
[19] Chitgar, N., *et al*., Investigation of a Novel Multigeneration System Driven by a SOFC for Electricity and Fresh Water Production, *Energy Conversion and Management*, *196* (2019), Sept., pp. 296-310
[20] Javed, A., *et al*., A Comparison of the Exergy Efficiencies of Various Heat-Integrated Distillation Columns, *Energies*, *15* (2022), 18, 6498
[21] Vojdani, M., *et al*., A Novel Triple Pressure HRSG Integrated with MED/SOFC/GT for Cogeneration of Electricity and Freshwater: Techno-Economic-Environmental Assessment, and Multi-Objective Optimization, *Energy Conversion and Management*, *233* (2021), Apr., 113876
[22] Han, X., *et al*., Thermodynamic Analysis and Life Cycle Assessment of Supercritical Pulverised Coal-Fired Power Plant Integrated with No. 0 Feedwater Pre-Heater under Partial Loads, *Journal of Cleaner Production*, *233* (2019), Oct., pp. 1106-1122
[23] Mojaver, P., *et al*., Multi-Objective Optimization of a Power Generation System Based SOFC using Taguchi/AHP/Topsis Triple Method, *Sustainable Energy Technologies and Assessments*, *38* (2020), Apr., 100674
[24] Tao, G., *et al*., Intermediate Temperature Solid Oxide Fuel Cell (IT-SOFC) Research and Development Activities at MSRI, *Proceedings*, Nineteenth Annual ACERC and ICES Conference, Provo, U., USA, 2005

Paper submitted: April 29, 2023
Paper revised: May 5, 2023
Paper accepted: June 10, 2023